# STRESS DISTRIBUTION IN THE HOLLOW STIFFENED HYBRID LAMINATED COMPOSITE PANELS IN SHIP STRUCTURES UNDER SINUSOIDAL LOADING

(DOI No: 10.3940/rina.ijme.2016.a2.346)

**M Sit**, **C Ray**, **D Biswas**, and **B Mandal**, Indian Institute of Engineering Science and Technology Shibpur, India

## SUMMARY

A simplified hollow stiffened hybrid laminated plate model has been developed for the marine structures. The detailed stress analysis through the thickness of the stiffened plate based on the higher order shear deformation theory has been carried out under sinusoidal loading. The hybrid laminates are made by wrapping the GFRP laminates with CFRP at the outermost layers of the stiffened panel. This hybridization technique can be an optimum solution from the point of view of cost reduction as well as enhancement of strength properties. The layer-wise stresses for the stiffened plate have been calculated in the present paper. A 3D polynomial curve fitting technique has been used to obtain higher accuracy and consistency in the computation of stresses. The computer code has been developed using MATLAB considering the plates as eight noded isoparametric plate bending element and the stiffener has been modeled as three noded isoparametric beam element. The stiffened panel has also been analysed using the ANSYS14.0 software package considering 2D model. The results obtained from the present formulation have been compared with those available in the published literature to validate the present formulation. The stiffened panels made of GFRP, CFRP and GFRP-CFRP hybrid laminates have been studied here. An extensive parametric study has been carried out with varying fibre content in the laminates.

## NOMENCLATURE

| | |
|---|---|
| u, v, w | displacements along x, y and z directions |
| $\theta x$, $\theta y$, $\zeta x$, $\zeta y$ | rotations of the normals to the mid-plane about x- and y-axes and their corresponding higher order terms in Taylor's series |
| $E_{11}$, $E_{22}$ | moduli of elasticity along and transverse to fiber direction |
| $G_{12}$, $G_{13}$, $G_{23}$ | rigidity moduli |
| $\upsilon_{12}$, $\upsilon_{13}$ | Poisson's ratios |
| $[N]_i$ | in plane force resultant |
| $[M]_i$ | bending moment resultant |
| $[Q]_i$ | transverse shear force resultant |
| $[P]_i$, $[R]_i$ | higher order stress resultant |
| [D] | rigidity matrix |
| $\{\varepsilon\}$ | strain vector |
| $(\overline{Q_{ij}})_k$ | compliance matrix of the individual laminae with different material properties |
| [B] | strain-displacement matrix |
| $[K_e]$ | stiffness matrix of the plate element |
| $a_{oh}$ | width of stiffener |
| $h_{oh}$ | depth of stiffener |
| $[\Lambda]$ | orientation matrix |
| [T] | transformation matrix |
| $[D_h]$ | rigidity matrix of the stiffener element |
| $\{\varepsilon_h\}$ | strain vector of the stiffener element |
| $[B_h]$ | strain-displacement matrix of the stiffener element |
| $[K_h]$ | stiffness matrix of the stiffener element |

## 1. INTRODUCTION

The stiffened structural configuration may be considered as the backbone of most of the marine structures. Several primary components like deck, hull, bottom and superstructures are modeled as stiffened plates. Due to the weight sensitivity of such structures, light weight constituent material is also of prime concern. The marine structures are subjected to wave loading of high frequency dynamic nature as well as low frequency quasi static nature. The quasi static wave induced load which is sinusoidal in nature acting on the ship structures may cause i) compression in plate and tension in stiffener ii) tension in plate and compression in stiffener and iii) in plane axial loading.

Several researchers have concentrated on the analysis of stiffened plates. Bedair and Troitsky [1] have presented the review of the analytical procedures for the analysis of stiffened plates. Hovichitr et al. [2] have presented an analytical formulation of rectangular plate with eccentric stiffener deriving fourth order differential equations. They have considered variational principle with natural boundary conditions. Fujikubo et al. [3] have developed a new simplified model for collapse analysis of stiffened plates. Their proposed stiffened plate model consists of ISUM plate elements and beam-column elements. The formulation of the plate element is performed by introducing accurate shape functions to simulate the buckling/plastic collapse behaviour of plate panels. Combining plate and beam-column elements allows for both local buckling of the plate panel and overall buckling of the stiffener. Sadek and Tawfik [4] have presented a refined higher-order displacement model for the studying the behaviour of concentrically and eccentrically stiffened laminated plates based on $C^0$

©2016: The Royal Institution of Naval Architects 

finite element discretization. The nine-noded isoparametric plate element with seven degrees of freedom at each node is used for the analysis. The stiffener element is a three noded isoparametric beam element with four degrees of freedom at each node. They have considered only rectangular stiffener. Ray and Satsangi [6] have developed a new generalized approach for the laminated composite plates with arbitrarily oriented stiffeners with various stiffener cross sections viz. rectangular, T, box and hat shapes using first order shear deformation theory. Barik and Mukhopadhyay [7] have developed a new stiffened plate model for arbitrary plates. A four noded stiffened plate element has been developed an isoparametric element for modelling arbitrary shaped plates. They have used a higher order element considering only usual degrees of freedom. Their study also includes only open section stiffeners. Qing et al. [8] have developed a mathematical model based on semi analytical solution of the state vector theory for the free vibration analysis of laminated stiffened plates with rectangular stiffener by separate consideration of plates and stiffeners. They have considered the first order shear deformation theory.

Several research works have already been reported on stiffened plates. However the investigation on the stress behaviour of hollow stiffened panel under sinusoidal loading is not reported in the literature. The study on the stress distribution in the stiffened panel is indispensable for the marine structures. The detailed stress analysis using higher order shear deformation theory of hollow stiffened laminated panel applicable to marine structures with closely spaced stiffeners with box configuration has not been reported till date. The detailed stress analysis (bending and shear) through the thickness of laminate can be obtained by considering higher order shear deformation theory.

Furthermore, application of GFRP-CFRP hybrid laminate to the stiffened plate panel developed in the present investigation is not reported earlier.

The objective of the present paper is to predict the stress distribution throughout the thickness of the stiffened plate and improvement in the stress behaviour due to hybridization. A hollow stiffened panel with closely spaced multiple stiffeners has been introduced in this purpose. The study has been carried out under the sinusoidal load causing compression in the plate and tension at the bottom of the stiffener. The hollow stiffened plates made of glass-epoxy (GFRP), carbon-epoxy (CFRP) and glass-carbon hybrid laminates have been studied here. The outermost layers of the stiffeners are made of carbon-epoxy material and the inner layers of the plate and the stiffener are with glass-epoxy material in case of hybrid laminate. This hybridization technique is a better choice of lamination scheme to strengthen GFRP laminates.

## 2. PRESENT FINITE ELEMENT FORMULATION FOR STIFFENED LAMINATED PANEL

The panel has been modeled as a plate stiffened with closely placed hollow multiple box stiffeners as shown in Figure 1.

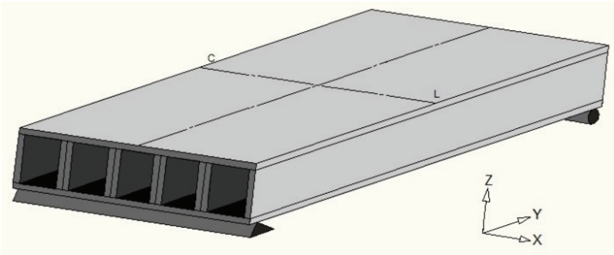


Figure 1: A Plate stiffened with closely spaced box stiffeners

The plate has been modeled as an eight noded isoparametric plate bending element with seven degrees of freedom per node viz. three translations (u, v, w) and two rotations ($\theta_x$ and $\theta_y$) and the corresponding higher order terms in Taylor's series ($\zeta_x$ and $\zeta_y$). The higher order shear deformation theory has been applied based on $C^0$ finite element model. The box sections have been modeled as the three noded beam elements with same number of degrees of freedom per node as in the plate element. The middle surface of the plate element has been considered as the reference plane and the rigidity of the stiffeners have been transferred to the middle surface of the plate.

### 2.1 FORMULATION OF PLATE ELEMENT

The stress resultants of the composite laminate are defined as:

$$\{F\}^T = \{N_x \quad N_y \quad N_s \quad M_x \quad M_y \quad M_s \quad P_x \quad P_y \quad P_s \quad Q_x \quad Q_y \quad R_x \quad R_y\} \tag{1}$$

and

$$\{F\} = [D]\{\varepsilon\} \tag{2}$$

The elements of the [$D$] matrix are defined as:

$$(A_{ij}, B_{ij}, D_{ij}, E_{ij}, F_{ij}, H_{ij}) = \sum_{k=1}^{n}\int_{z_{k-1}}^{z_k} \left(\overline{Q}_{ij}\right)_k (1, z, z^2, z^3, z^4, z^6)dz, \quad i, j = x, y, s \tag{3}$$

and

$$\left(A_{ij}^z, B_{ij}^z, D_{ij}^z\right) = \sum_{k=1}^{n}\int_{z_{k-1}}^{z_k} \left(\overline{Q_{ij}}\right)_k (1, z^2, z^4)dz \quad i, j = x, y, s \tag{4}$$

 ©2016: The Royal Institution of Naval Architects

The nodal displacements at any node 'r' of the plate element can be expressed as:

$$\{\delta_r\}^T = \{u_r \quad v_r \quad w_r \quad \theta_{xr} \quad \theta_{yr} \quad \zeta_{xr} \quad \zeta_{yr}\} \tag{5}$$

The displacements at any point within the plate element can be expressed in terms of the nodal displacements as:

$$\{u \; v \; w \; \theta_x \; \theta_y \; \zeta_x \; \zeta_y\}^T = \sum_{r=1}^{8} [N_r][I_8]\{u_r \; v_r \; w_r \; \theta_{xr} \; \theta_{yr} \; \zeta_{xr} \; \zeta_{yr}\}^T \tag{6}$$

where $[N_r]$ is the shape function matrix. The element stiffness matrix for the plate element is given by

$$[K_e] = \int_{-1}^{1}\int_{-1}^{1} [B]^T [D][B]|J| d\xi d\eta \tag{7}$$

## 2.2 FORMULATION OF STIFFENER ELEMENT

The stiffener cross section has been considered as a box section with equal top and bottom width as shown in Figure 3. The nodes of the stiffener element need not merge with the nodes of the plate element. The stiffener element has been developed by considering an arbitrarily oriented box shaped stiffener as shown in Figure 2. The stiffener is modeled as three noded beam element in which modulus-weighted centroid is assumed to be at the centre line of the section.

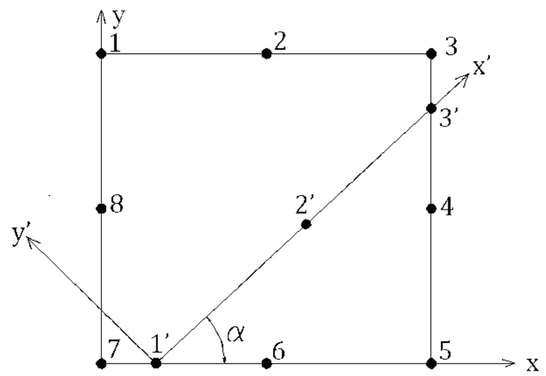


1, 2, 3…. 8 plate nodes
1′, 2′, 3′ stiffener nodes

Figure 2: Nodes and axis system of plate and stiffener elements

The coordinates of the beam element can be expressed as: $x' = \sum_{i=1}^{3} N_i x_i'$ (8)

where, $N_i's$ are the shape functions of the stiffener element can be written as:

$$\begin{aligned} N_1 &= -\xi(1-\xi)/2 \\ N_2 &= (1-\xi^2)/2 \\ N_3 &= \xi(1+\xi)/2 \end{aligned} \tag{9}$$

The nodal displacements at any node 'i' of the three noded beam element can be expressed as:

$$\{\delta_{hi}'\}^T = \{u_i' \quad v_i' \quad w_i' \quad \theta_{xi}' \quad \theta_{yi}' \quad \zeta_{xi}' \quad \zeta_{yi}'\} \tag{10}$$

The displacements at any point of the stiffener element can be expressed in terms of the nodal displacements as:

$$\begin{Bmatrix} u' \\ v' \\ w' \\ \theta_x' \\ \theta_y' \\ \zeta_x' \\ \zeta_y' \end{Bmatrix} = \sum_{i=1}^{3} [N_i][I_3] \begin{Bmatrix} u_i' \\ v_i' \\ w_i' \\ \theta_{xi}' \\ \theta_{yi}' \\ \zeta_{xi}' \\ \zeta_{yi}' \end{Bmatrix} \tag{11}$$

The displacements at any point of the stiffener element in terms of the displacements of the plate with respect to plate axis system are given by:

$$\begin{aligned} u' &= u\,cos\alpha + v\,sin\alpha \\ v' &= -u sin\alpha + v cos\alpha = 0 \\ w' &= w \\ \theta_x' &= \theta_x cos\alpha + \theta_y sin\alpha \\ \theta_y' &= -\theta_x\,sin\alpha + \theta_y\,cos\alpha \\ \zeta_x' &= \zeta_x\,cos\alpha + \zeta_y\,sin\alpha \\ \zeta_y' &= -\zeta_x\,sin\alpha + \zeta_y\,cos\alpha \end{aligned} \tag{12}$$

where, α is the angle between x axis of the plate and $x'$ axis of the stiffener as shown in Figure 2.

The Eqn. (12) can be re-written as:

$$\sum_{i=1}^{3}\{\delta_h\}_i = [\Lambda]\sum_{i=1}^{3}\{\delta\}_i \tag{13}$$

where,

$$[\Lambda] = \begin{bmatrix} [\Lambda]_1 & & \\ & [\Lambda]_2 & \\ & & [\Lambda]_3 \end{bmatrix} \tag{14}$$

and

$$[\Lambda]_i = \begin{bmatrix} c & s & 0 & 0 & 0 & 0 & 0 \\ -s & c & 0 & 0 & 0 & 0 & 0 \\ 0 & 0 & 1 & 0 & 0 & 0 & 0 \\ 0 & 0 & 0 & c & s & 0 & 0 \\ 0 & 0 & 0 & -s & c & 0 & 0 \\ 0 & 0 & 0 & 0 & 0 & c & s \\ 0 & 0 & 0 & 0 & 0 & -s & c \end{bmatrix} \tag{15}$$

where, $c = cos\alpha$ and $s = sin\alpha$ .

The displacement field at any point within the stiffener placed along x' direction is given by:

$$\begin{Bmatrix} U' \\ V' \\ W' \end{Bmatrix} = \begin{Bmatrix} u' - z'\theta_x' - z'^2\psi_x' - z'^3\zeta_x' \\ -z'\theta_y' - z'^2\psi_y' - z'^3\zeta_y' \\ w' + y'\theta_y' + y'\zeta_y' \end{Bmatrix} \tag{16}$$

where u' and w' are the displacements and $\theta_{x'}$ and $\theta_{y'}$ the rotations of the normal to the undeformed midplane of the plate parallel to the local axis system of the stiffener.

The strain components at any point within the stiffener is given by:

$$\begin{Bmatrix} \varepsilon_x' \\ \varepsilon_s' \\ \varepsilon_{x'z'} \end{Bmatrix} = \begin{Bmatrix} \dfrac{\partial U'}{\partial x'} \\ \dfrac{\partial U'}{\partial y'} + \dfrac{\partial V'}{\partial x'} \\ \dfrac{\partial U'}{\partial z'} + \dfrac{\partial W'}{\partial x'} \end{Bmatrix} = \begin{Bmatrix} \dfrac{\partial u'}{\partial x'} - z'\dfrac{\partial \theta_x'}{\partial x'} - z'^3\dfrac{\partial \zeta_x'}{\partial x'} \\ \dfrac{\partial u'}{\partial y'} - z'(\dfrac{\partial \theta_x'}{\partial y'} + \dfrac{\partial \theta_y'}{\partial x'}) - z'^3(\dfrac{\partial \zeta_x'}{\partial y'} + \dfrac{\partial \zeta_y'}{\partial x'}) \\ (\dfrac{\partial w'}{\partial x'} - \theta_x') - 3z'^2\zeta_x' + y'(\dfrac{\partial \theta_y'}{\partial x'} + \dfrac{\partial \zeta_y'}{\partial x'}) \end{Bmatrix} \tag{17}$$

The strain components developed in the stiffener element with respect to the reference axis system of the stiffener element are

$$\{\varepsilon_h\} = \begin{Bmatrix} \dfrac{\partial u'}{\partial x'} & -\dfrac{\partial \theta_x'}{\partial x'} & -\dfrac{\partial \zeta_x'}{\partial x'} & (\dfrac{\partial \theta_w'}{\partial x'} - \partial\theta_x') & -3\zeta_x' & (\dfrac{\partial \theta_y'}{\partial x'} + \dfrac{\partial \zeta_y'}{\partial x'}) \end{Bmatrix}^T \tag{18}$$

The strain-displacement relationship of the stiffener element is given by

$$\{\varepsilon_h\} = \sum_{i=1}^{3} [B_h]_i \{\delta_h\}_i \tag{19}$$

where,

$$[B_h]_i = \begin{bmatrix} \dfrac{\partial N_i}{\partial x'} & 0 & 0 & 0 & 0 & 0 & 0 \\ 0 & 0 & 0 & -\dfrac{\partial N_i}{\partial x'} & 0 & 0 & 0 \\ 0 & 0 & 0 & 0 & 0 & -\dfrac{\partial N_i}{\partial x'} & 0 \\ 0 & 0 & \dfrac{\partial N_i}{\partial x'} & -N_i & 0 & 0 & 0 \\ 0 & 0 & 0 & 0 & 0 & -3N_i & 0 \\ 0 & 0 & 0 & 0 & \dfrac{\partial N_i}{\partial x'} & 0 & \dfrac{\partial N_i}{\partial x'} \end{bmatrix} \tag{20}$$

The nodes of the stiffener element exist within the plate element. The nodal displacements of the stiffener element in terms of the nodal displacements of the plate element can be expressed as:

$$\sum_{i=1}^{3} \{\delta_h\}_i = [\Lambda][T] \sum_{i=1}^{3} \{\delta_r\}_i \tag{21}$$

The matrix form of the transformation $[T]$ is written as:

$$[T] = \sum_{i=1}^{3}\sum_{r=1}^{8} = \begin{bmatrix} [N_{ir}] & & & & & & \\ & [N_{ir}] & & & & & \\ & & [N_{ir}] & & & & \\ & & & [N_{ir}] & & & \\ & & & & [N_{ir}] & & \\ & & & & & [N_{ir}] & \\ & & & & & & [N_{ir}] \end{bmatrix} \tag{22}$$

where, $N_{ir}$ is the shape function at the r$^{th}$ node of the plate element corresponding to the i$^{th}$ node of the stiffener element.

The stiffness matrix of the three noded beam element is calculated as:

$$[K_h] = \int_{x'} [T]^T [\Lambda]^T [B_h]^T [D_h][B_h][\Lambda][T]\, dx' \tag{23}$$

or, $$[K_h] = \int_{x'} [T]^T [\Lambda]^T [\bar{K}_h][\Lambda][T]\, dx' \tag{24}$$

So, $$[\bar{K}_h] = [B_h]^T [D_h][B_h] \tag{25}$$

2.3 RIGIDITY MATRIX OF STIFFENER ELEMENT

In the present investigation, box shaped stiffeners are considered. The stress resultants of the stiffener of any general shape are given by:

$$\{F_h\}^T = \{N_h \quad M_h \quad P_h \quad Q_h \quad R_h \quad T_h\} \tag{26}$$

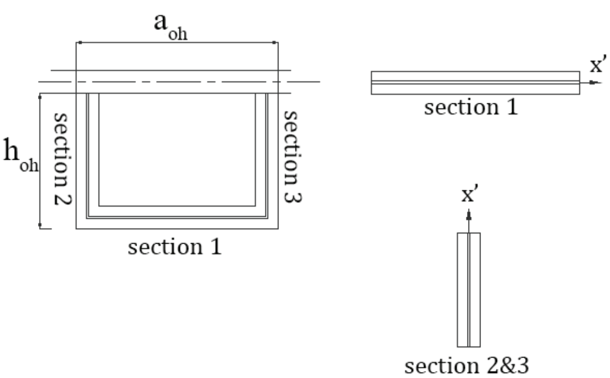


Figure 3: The box stiffener with two vertical and one horizontal section

 ©2016: The Royal Institution of Naval Architects

For a box shaped stiffener, the stress resultants are given by:

$$\begin{aligned}
N_h &= N_h^1 + N_h^2 + N_h^3 \\
M_h &= M_h^1 + M_h^2 + M_h^3 \\
P_h &= P_h^1 + P_h^2 + P_h^3 \\
Q_h &= Q_h^1 + Q_h^2 + Q_h^3 \\
R_h &= R_h^1 + R_h^2 + R_h^3 \\
T_h &= T_h^1 + T_h^2 + T_h^3
\end{aligned} \tag{27}$$

Where, $N_h$ is the force resultant, $M_h$ is the moment resultant, $Q_h$ is the shear force resultant and $P_h$ and $R_h$ are the higher order stress resultant of the stiffener element. $T_h$ is the stress resultant related to torsional rigidity.

Where

$$N_h^1 = \int_{z_k'}^{z_{k+1}'}\int_{-b_h/2}^{b_h/2} Q_{x'x'}\left(\frac{\partial u'}{\partial x'} - z'\frac{\partial \theta_x'}{\partial x'} - z'^3\frac{\partial \zeta_x'}{\partial x'}\right)dy'dz' \tag{28}$$

$$\begin{aligned}N_h^2 = &\int_{y_k'}^{y_{k+1}'}\int_{h_1}^{h_2} Q_{x'x'}\left(\frac{\partial u'}{\partial x'} - z'\frac{\partial \theta_x'}{\partial x'} - z'^3\frac{\partial \zeta_x'}{\partial x'}\right)dy'dz' - \int_{y_k'}^{y_{k+1}'}\int_{h_1}^{h_2} Q_{x's'}\Big\{\left(\frac{\partial w'}{\partial x'} - \theta_x'\right) \\ &-3z'^2\zeta_x' + y'\left(\frac{\partial \theta_y'}{\partial x'} + \frac{\partial \zeta_y'}{\partial x'}\right)\Big\}dy'dz'\end{aligned} \tag{29}$$

$$\begin{aligned}N_h^3 = &\int_{y_k'}^{y_{k+1}'}\int_{h_1}^{h_2} Q_{x'x'}\left(\frac{\partial u'}{\partial x'} - z'\frac{\partial \theta_x'}{\partial x'} - z'^3\frac{\partial \zeta_x'}{\partial x'}\right)dy'dz' + \int_{y_k'}^{y_{k+1}'}\int_{h_1}^{h_2} Q_{x's'}\Big\{\left(\frac{\partial w'}{\partial x'} - \theta_x'\right) \\ &-3z'^2\zeta_x' + y'\left(\frac{\partial \theta_y'}{\partial x'} + \frac{\partial \zeta_y'}{\partial x'}\right)\Big\}dy'dz'\end{aligned} \tag{30}$$

$$M_h^1 = \int_{z_k'}^{z_{k+1}'}\int_{-b_h/2}^{b_h/2} Q_{x'x'}\left(\frac{\partial u'}{\partial x'} - z'\frac{\partial \theta_x'}{\partial x'} - z'^3\frac{\partial \zeta_x'}{\partial x'}\right)z'dy'dz' \tag{31}$$

$$\begin{aligned}M_h^2 = &\int_{y_k'}^{y_{k+1}'}\int_{h_1}^{h_2} Q_{x'x'}\left(\frac{\partial u'}{\partial x'} - z'\frac{\partial \theta_x'}{\partial x'} - z'^3\frac{\partial \zeta_x'}{\partial x'}\right)z'dy'dz' - \int_{y_k'}^{y_{k+1}'}\int_{h_1}^{h_2} Q_{x's'}\Big\{\left(\frac{\partial w'}{\partial x'} - \theta_x'\right) \\ &-3z'^2\zeta_x' + y'\left(\frac{\partial \theta_y'}{\partial x'} + \frac{\partial \zeta_y'}{\partial x'}\right)\Big\}z'dy'dz'\end{aligned} \tag{32}$$

$$\begin{aligned}M_h^3 = &\int_{y_k'}^{y_{k+1}'}\int_{h_1}^{h_2} Q_{x'x'}\left(\frac{\partial u'}{\partial x'} - z'\frac{\partial \theta_x'}{\partial x'} - z'^3\frac{\partial \zeta_x'}{\partial x'}\right)z'dy'dz' + \int_{y_k'}^{y_{k+1}'}\int_{h_1}^{h_2} Q_{x's'}\Big\{\left(\frac{\partial w'}{\partial x'} - \theta_x'\right) \\ &-3z'^2\zeta_x' + y'\left(\frac{\partial \theta_y'}{\partial x'} + \frac{\partial \zeta_y'}{\partial x'}\right)\Big\}z'dy'dz'\end{aligned} \tag{33}$$

$$P_h^1 = \int_{z_k'}^{z_{k+1}'}\int_{-b_h/2}^{b_h/2} Q_{x'x'}\left(\frac{\partial u'}{\partial x'} - z'\frac{\partial \theta_x'}{\partial x'} - z'^3\frac{\partial \zeta_x'}{\partial x'}\right)z'^3dy'dz' \tag{34}$$

$$\begin{aligned}P_h^2 = &\int_{y_k'}^{y_{k+1}'}\int_{h_1}^{h_2} Q_{x'x'}\left(\frac{\partial u'}{\partial x'} - z'\frac{\partial \theta_x'}{\partial x'} - z'^3\frac{\partial \zeta_x'}{\partial x'}\right)z'^3dy'dz' - \int_{y_k'}^{y_{k+1}'}\int_{h_1}^{h_2} Q_{x's'}\Big\{\left(\frac{\partial w'}{\partial x'} - \theta_x'\right) \\ &-3z'^2\zeta_x' + y'\left(\frac{\partial \theta_y'}{\partial x'} + \frac{\partial \zeta_y'}{\partial x'}\right)\Big\}z'^3dy'dz\end{aligned} \tag{35}$$

$$\begin{aligned}P_h^3 = &\int_{y_k'}^{y_{k+1}'}\int_{h_1}^{h_2} Q_{x'x'}\left(\frac{\partial u'}{\partial x'} - z'\frac{\partial \theta_x'}{\partial x'} - z'^3\frac{\partial \zeta_x'}{\partial x'}\right)z'^3dy'dz' + \int_{y_k'}^{y_{k+1}'}\int_{h_1}^{h_2} Q_{x's'}\Big\{\left(\frac{\partial w'}{\partial x'} - \theta_x'\right) \\ &-3z'^2\zeta_x' + y'\left(\frac{\partial \theta_y'}{\partial x'} + \frac{\partial \zeta_y'}{\partial x'}\right)\Big\}z'^3dy'dz'\end{aligned} \tag{36}$$

$$Q_h^1 = \int_{z_k'}^{z_{k+1}'}\int_{-b_h/2}^{b_h/2} Q_{x'x'}^{z}\Big\{\left(\frac{\partial w'}{\partial x'} - \theta_x'\right) - 3z'^2\zeta_x' + y'\left(\frac{\partial \theta_y'}{\partial x'} + \frac{\partial \zeta_y'}{\partial x'}\right)\Big\}dy'dz' \tag{37}$$

$$\begin{aligned}Q_h^2 = &-\int_{y_k'}^{y_{k+1}'}\int_{h_1}^{h_2} Q_{x's'}\left(\frac{\partial u'}{\partial x'} - z'\frac{\partial \theta_x'}{\partial x'} - z'^3\frac{\partial \zeta_x'}{\partial x'}\right)dy'dz' + \int_{y_k'}^{y_{k+1}'}\int_{h_1}^{h_2} Q_{s's'}\Big\{\left(\frac{\partial w'}{\partial x'} - \theta_x'\right) \\ &-3z'^2\zeta_x' + y'\left(\frac{\partial \theta_y'}{\partial x'} + \frac{\partial \zeta_y'}{\partial x'}\right)\Big\}dy'dz'\end{aligned} \tag{38}$$

$$\begin{aligned}Q_h^3 = &\int_{y_k'}^{y_{k+1}'}\int_{h_1}^{h_2} Q_{x's'}\left(\frac{\partial u'}{\partial x'} - z'\frac{\partial \theta_x'}{\partial x'} - z'^3\frac{\partial \zeta_x'}{\partial x'}\right)dy'dz' + \int_{y_k'}^{y_{k+1}'}\int_{h_1}^{h_2} Q_{s's'}\Big\{\left(\frac{\partial w'}{\partial x'} - \theta_x'\right) \\ &-3z'^2\zeta_x' + y'\left(\frac{\partial \theta_y'}{\partial x'} + \frac{\partial \zeta_y'}{\partial x'}\right)\Big\}dy'dz'\end{aligned} \tag{39}$$

$$R_h^1 = \int_{z_k'}^{z_{k+1}'}\int_{-b_h/2}^{b_h/2} Q_{x'x'}^{z}\Big\{\left(\frac{\partial w'}{\partial x'} - \theta_x'\right) - 3z'^2\zeta_x' + y'\left(\frac{\partial \theta_y'}{\partial x'} + \frac{\partial \zeta_y'}{\partial x'}\right)\Big\}z'^2dy'dz' \tag{40}$$

$$\begin{aligned}R_h^2 = &-\int_{y_k'}^{y_{k+1}'}\int_{h_1}^{h_2} Q_{x's'}\left(\frac{\partial u'}{\partial x'} - z'\frac{\partial \theta_x'}{\partial x'} - z'^3\frac{\partial \zeta_x'}{\partial x'}\right)z'^2dy'dz' + \int_{y_k'}^{y_{k+1}'}\int_{h_1}^{h_2} Q_{s's'}\Big\{\left(\frac{\partial w'}{\partial x'} - \theta_x'\right) \\ &-3z'^2\zeta_x' + y'\left(\frac{\partial \theta_y'}{\partial x'} + \frac{\partial \zeta_y'}{\partial x'}\right)\Big\}z'^2dy'dz'\end{aligned} \tag{41}$$

$$\begin{aligned}R_h^3 = &\int_{y_k'}^{y_{k+1}'}\int_{h_1}^{h_2} Q_{x's'}\left(\frac{\partial u'}{\partial x'} - z'\frac{\partial \theta_x'}{\partial x'} - z'^3\frac{\partial \zeta_x'}{\partial x'}\right)z'^2dy'dz' + \int_{y_k'}^{y_{k+1}'}\int_{h_1}^{h_2} Q_{s's'}\Big\{\left(\frac{\partial w'}{\partial x'} - \theta_x'\right) \\ &-3z'^2\zeta_x' + y'\left(\frac{\partial \theta_y'}{\partial x'} + \frac{\partial \zeta_y'}{\partial x'}\right)\Big\}z'^2dy'dz'\end{aligned} \tag{42}$$

2.3 (a) Torsional rigidity of the box stiffener

The box stiffener induces a considerable amount of torsional rigidity due to its closed attachment with the plate. The box stiffener is considered as a hollow section to compute the torsional rigidity accurately. The torsional rigidity is calculated in the following manner,

$J_h$ = ($J_h$ of the section with outer profile of the box stiffener - $J_h$ of the inner profile of the box stiffener)

## 3. FORMULATION OF ELEMENT LOAD VECTOR

The sinusoidal load is considered as acting perpendicular to the plane of the plate over the surface. The load induces compression on the plate surface and tension at the stiffener bottom.

## 4. COMPUTATION OF STRESS

The linear static analysis has been carried out under sinusoidal loading. The stress analysis through the thickness of the laminate has been carried out for the stiffened plate model considering higher order shear deformation theory. The stresses have been computed at the gauss points of the elements. The nodal stresses have been computed by the 3D polynomial curve fitting technique [8, 9] to obtain accuracy and consistency in the stress value.

## 5. FINITE ELEMENT FORMULATION USING ANSYS

The SHELL281 element available in the ANSYS 14 software package has been used for 2D model considering the first order shear deformation theory to model the hollow panel.

### 5.1 MODELING AND ANALYSIS OF HOLLOW STIFFEND PLATES

The stiffened panel has been developed by considering one plate at top and another plate at bottom with six vertical blade stiffeners placed between two plates as shown in Figure 4. Two edges parallel to X axis of the plate is simply supported (one end pinned and other end roller supported) and other two edges are free. The modeling of the hollow stiffened plates using ANSYS is shown in Figure 4.

## 6. RESULTS AND DISCUSSIONS

### 6.1 SIMPLY SUPPORTED CROSS PLY SQUARE LAMINATED PLATE UNDER SINUSOIDAL LOAD

A simply supported square symmetric cross ply [0°/90°/90°/0°] laminated plate subjected to a sinusoidal load P=q sin(πx/a) sin(πx/b) has been studied here. Length to thickness ratio of the laminate is a/h=10. The material properties of each GFRP lamina are: $E_1/E_2=25$; $G_{12}=G_{13}=0.5E_2$; $G_{23}=0.2E_2$; $\nu_{12}=0.25$. Thai et al. (10) have solved the same problem using node-based smoothing discrete shear gap method with higher order shear deformation plate theory. They have used four noded rectangular element. The stresses obtained from the present finite element formulation have been compared with those available in the published literature to validate the same. The normalized stresses for the symmetric cross ply square plate is defined as:

$$\bar{\sigma}_x = \frac{h^2}{qa^2}\sigma_x \text{ and } \bar{\sigma}_y = \frac{h^2}{qa^2}\sigma_y$$

The normalized stresses through the thickness of the laminated plates are compared and presented in Figure 5. The variation of stresses through the thickness of the plate obtained from the present higher order shear deformation theory and those obtained from Thai et al. [10] tally very well.

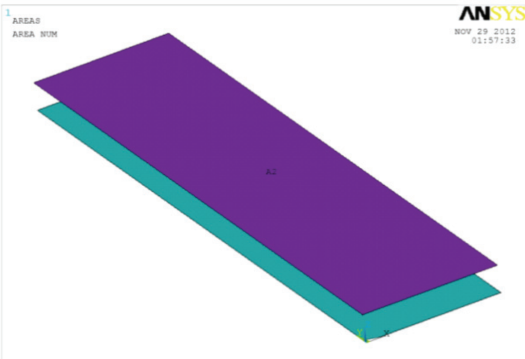


(a) Top and bottom plate of the panel

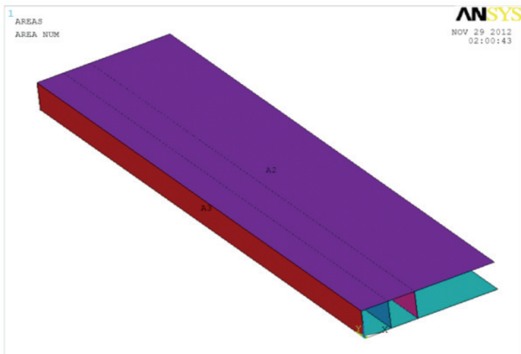


(b) The incomplete panel model with 3stiffeners

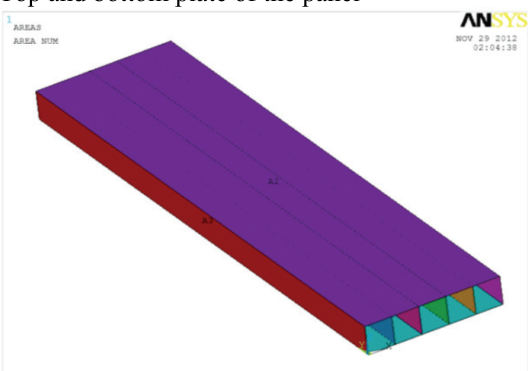


(c) The stiffened laminated panel

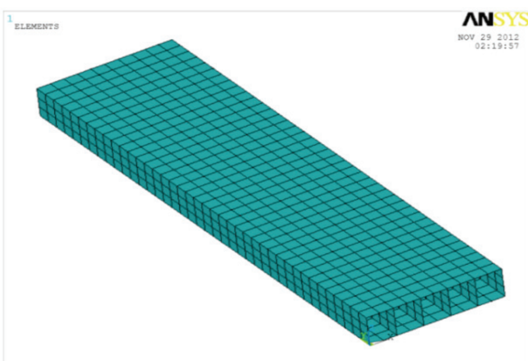


(d) Mesh division of the stiffened plate

Figure 4: Modeling of stiffened panel using ANSYS 14.0



*©2016: The Royal Institution of Naval Architects*

### 6.2 HOLLOW STIFFENED GFRP LAMINATED PLATE UNDER SINUSOIDAL LOAD

A hollow stiffened laminated plate panel of dimension 500mm × 500mm and made of E-Glass/Epoxy cross-ply laminates of thickness 50 mm has been considered for this analysis. The width of the hollow stiffener is 100mm and depth is 125mm. The plate and the stiffener laminates consist of four layers of equal thickness. The studies have been carried out for various fibre contents. The material properties of the GFRP ply are considered as: $E_1$=41 GPa; $E_2$=12 GPa; $G_{12}$=5.5 GPa; $G_{23}$=3.5 GPa; $\nu_{12}$=0.28; $\nu_{23}$=0.4. The material properties of the CFRP ply are considered as: $E_1$=138 GPa; $E_2$= 11 GPa; $G_{12}$=5.5 GPa; $G_{23}$=3.93 GPa; $\nu_{12}$=0.278; $\nu_{23}$=0.4. A single sinusoidal load is applied across the stiffener. The boundary conditions for the stiffened panel has been taken as two shorter edges simply supported (one end pinned and roller support on another end) and other two edges are free. The maximum deflections for GFRP, CFRP and hybrid (carbon and glass fibres) laminates are computed by the present formulation and the results are compared with those obtained in ANSYS. The deflections obtained from present higher order shear deformation theory have been compared with those obtained from ANSYS (FSDT) to predict the effect of HSDT in the formulation. The maximum deflections for all types of laminates are presented in Table 1 and Table 2.

Table 1: Maximum deflection (in mm) of the laminated stiffened panels subjected to sinusoidal load for symmetric cross ply laminates

| | **GFRP** | **CFRP** | **Hybrid** |
|---|---|---|---|
| **FSDT** | 0.0435 | 0.0098 | 0.0153 |
| **ANSYS** | 0.0482 | 0.0091 | 0.0168 |
| **HSDT** | 0.0593 | 0.0129 | 0.0201 |

Table 2: Maximum deflection (in mm) of the laminated stiffened panel subjected to sinusoidal load for anti-symmetric cross ply

| | **GFRP** | **CFRP** | **Hybrid** |
|---|---|---|---|
| **FSDT** | 0.0725 | 0.0192 | 0.0358 |
| **ANSYS** | 0.0772 | 0.0200 | 0.0390 |
| **HSDT** | 0.0819 | 0.0221 | 0.0431 |

The results presented in Table 1 and Table 2 reflect that the first order shear deformation theory underestimates the deflection. The comparisons of deflection for various laminates presented in Table 1 and Table 2 show that the hybridization technique by replacing the outermost layers with carbon laminae can reduce the displacement around 65% in case of symmetric cross ply and 49% in case of antisymmetric cross ply laminates.

The normal and shear stresses in normalized term have been computed for various lamination schemes and are presented in Figure 6 and Figure 7. The study using ANSYS has been carried out considering first order shear deformation theory. No study is reported in the published literature on the stress behaviour of laminated stiffened plate using the higher order shear deformation theory.

The normal and shear stress distributions in the symmetric cross ply stiffened laminates across the thickness of laminated plate have been presented in Figure 6. It is observed from the Figure 6 that the stress behaviour can also be improved significantly by wrapping the GFRP laminate with CFRP laminae at top and bottom surfaces of the stiffened plate instead of using only CFRP which is too costly. The stress distributions of the anti-symmetric cross ply laminates presented in Figure 7 also show the same trend of improvement in the stress behaviour with hybrid laminates. The effect of hybridization on the shear stress $\tau_{yz}$ for antisymmetric cross ply stiffened laminate is less significant. It is also found that hybridization makes more significant change in the normal stresses at the outer layers than the middle layers of the laminates whereas the change in shear stresses is more prominant at the middle part of the laminate.

## 7. CONCLUSIONS

The hollow stiffened hybrid laminated panels for the marine structures have been studied under the sinusoidal loading. The parametric studies on the stiffened laminated plates show that wrapping of glass-epoxy laminates with carbon-epoxy lamina improves the behaviour of the stiffened panel under sinusoidal loading condition significantly. The cost reduction of the high performance marine structure can be achieved by using the efficient hybridization technique developed in the present study instead of using fully carbon fibres in a laminate. The present study shows that use of carbon fabric may reduce 77% displacement with reference to glass fabric. Whereas CFRP-GFRP hybrid laminate developed in the present formulation can reduce the deflection by 65% in case of symmetric cross ply and 49% in case of antisymmetric cross ply laminates. The cost of hybrid laminate is only about 1.75 times more than that of the glass fabric. Whereas carbon fibre is much more costlier than glass fibres. Henceforth, the hybridization technique used for the stiffened panels is considerably cost effective and beneficial from the point of view of strengthening effect.

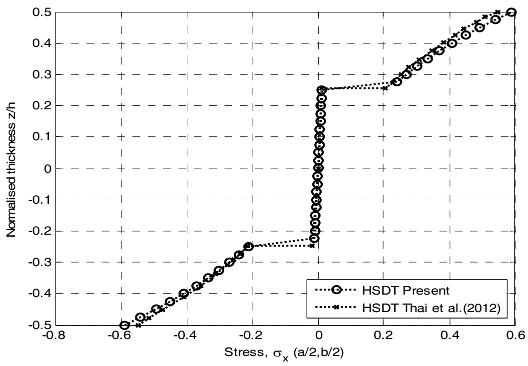


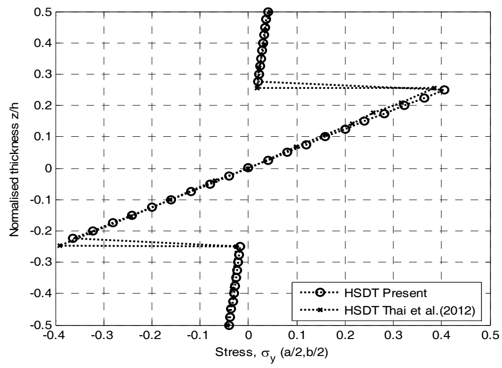


(a) Normal stress in x-direction ($s_x$) (b) Normal stress in y-direction ($s_y$)

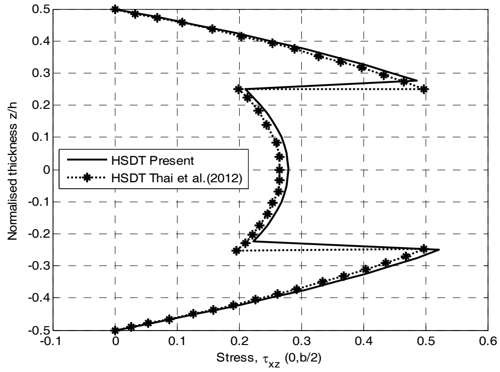


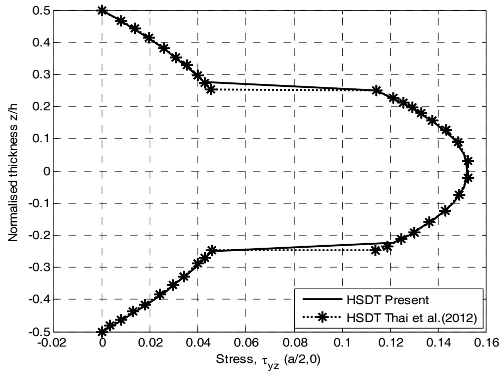


(c) Transverse shear stress ($\tau_{xz}$) (d) Transverse shear stress ($\tau_{yz}$)

Figure 5: The distribution of stresses through the thickness of plate under sinusoidal load

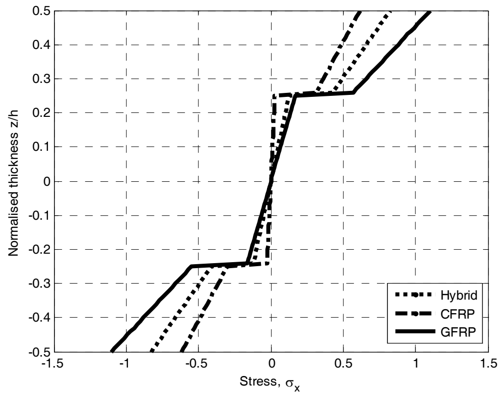


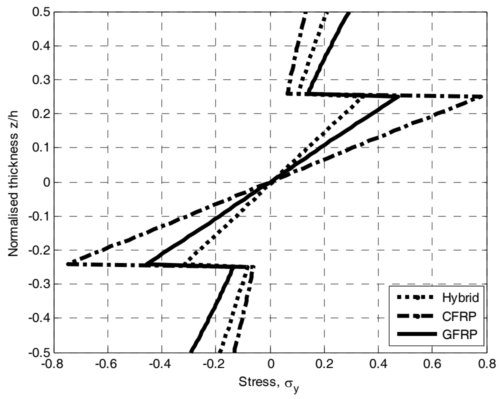


(a) Normal stress in x-direction ($s_x$) (b) Normal stress in y-direction ($s_y$)

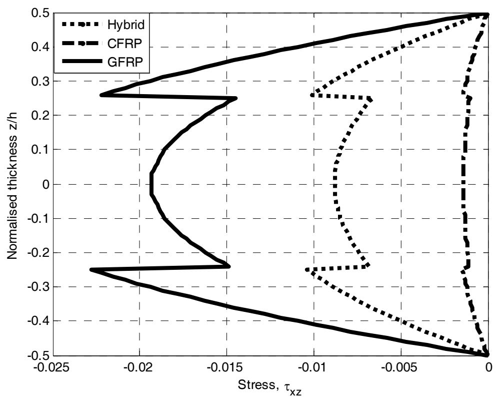


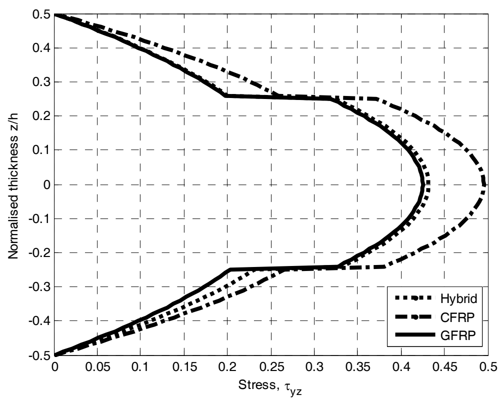


(c) Transverse shear stress ($\tau_{xz}$) (d) Transverse shear stress ($\tau_{yz}$)

Figure 6: The stress distribution through the thickness of plate for symmetric cross ply stiffened laminate

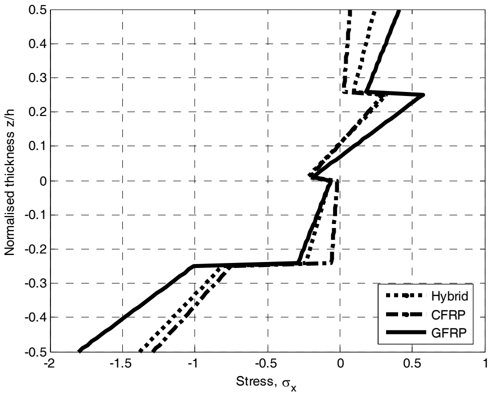


(a) Normal stress in x-direction ($s_x$)

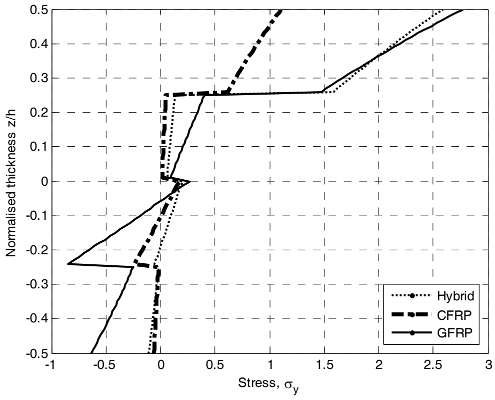


(b) Normal stress in y-direction ($s_y$)

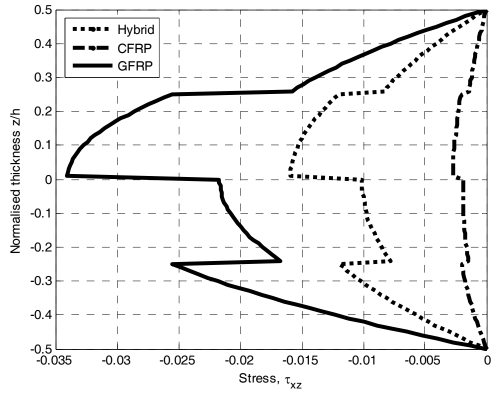


(c) Transverse shear stress ($\tau_{xz}$)

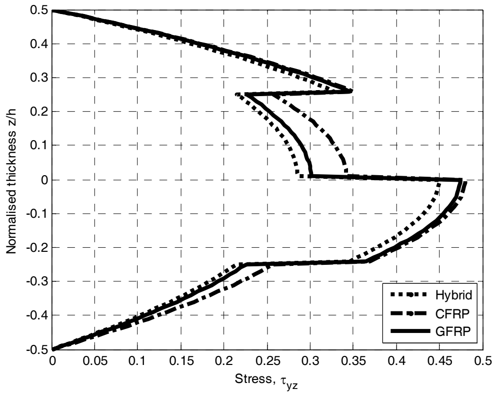


(d) Transverse shear stress ($\tau_{yz}$)

Figure 7: The stress distribution through the thickness of plate for anti-symmetric cross ply stiffened laminate

## 8. ACKNOWLEDGEMENT

The study included in this paper is funded by the Ministry of Shipping, Government of India.

## 9. REFERENCES

1. BEDAIR, O., AND TROITSKY, M. S., "Industrial Applications of Stiffened Plate Assemblies," *Technical Report for Natural Sciences and Engineering Research Council of Canada.* 1999
2. HOVICHITR, I., KARASUDHI, P., NISHINO, F., and LEE, S. L., "A Rational Analysis of Plates With Eccentric Stiffeners," "*IABSE Proceedings" No. P-4/77, pp. 1–14.* 1977
3. FUJIKUBO, M., and KAEDING, P., "New Simplified Approach to Collapse Analysis of Stiffened Plates," *Mar. Struct., 15 (3), pp. 251–283.* 2002
4. SADEK, E., and TAWFIK, S., "A Finite Element Model for the Analysis of Stiffened Laminated Plates," *Comput. Struct., 75 (4), pp. 369–383.* 2000
5. RAY, C. and SATSANGI S.K., Finite element analysis of laminated hat stiffened plates". *Journal of Reinforced Plastic and Composites, 15(12), pp. 1174-1193.* 1996
6. BARIK, M., and MUKHOPADHYAY, M., "A New Stiffened Plate Element for the Analysis of Arbitrary Plates," *Thin-Walled Struct., 40 , pp. 625–632.* 2002
7. QING, G., QIU JIAJUN and YANHONG L., "Free vibration analysis of stiffened laminated plates", *Int. J. Solids & Structures, 43(6), pp. 1357-1371.* 2006
8. BROWN L. D. and WONG W. K., "An algorithmic construction of optimal minimax designs for heteroscedastic linear model", *Journal of Statistical Planning and Inference, 85, pp. 103-114.* 2000
9. GAFFKE N. and HEILIGERS B., "Algorithms for optimal design with application to multiple polynomial regression", *Metrika, 42, pp. 173-190.* 1995
10. THAI CH, TRAN LV, TRAN DT, THOI TN and XUAN HN. Analysis of laminated composite plates using higher-order shear deformation plate theory and node-based smoothed discrete shear gap method. *Appl Math Model 2012;36:5657-5677.*